THE JOURNAL OF PHYSICAL CHEMISTRY B

ARTICLE

pubs.acs.org/JPCB

Conservation of Spin Polarization during Triplet−Triplet Energy Transfer in Reconstituted Peridinin−Chlorophyll−Protein Complexes

Marilena Di Valentin,*[,†] Claudia Tait,[†] Enrico Salvadori,[†] Stefano Ceola,[†] Hugo Scheer,[‡] Roger G. Hiller,[§] and Donatella Carbonera[†]

[†]Dipartimento di Scienze Chimiche, Università degli Studi di Padova, via Marzolo 1, 35131 Padova, Italy

[‡]Department Biologie I-Botanik, Ludwig-Maximilians-Universität München, Menziger Strasse 67, D-80638 München, Germany

[§]Department of Biological Sciences, Macquarie University, North Ryde, NSW 2109, Australia

Supporting Information

ABSTRACT: Peridinin−chlorophyll−protein (PCP) complexes, where the N-terminal domain of native PCP from *Amphidinium carterae* has been reconstituted with different chlorophyll (Chl) species, have been investigated by time-resolved EPR in order to elucidate the details of the triplet−triplet energy transfer (TTET) mechanism. This spectroscopic approach exploits the concept of spin conservation during TTET, which leads to recognizable spin-polarization effects in the observed time-resolved EPR spectra. The spin polarization produced at the acceptor site (peridinin) depends on the initial polarization of the donor (chlorophyll) and on the relative geometric arrangement of the donor−acceptor spin axes. A variation of the donor triplet state properties in terms of population probabilities or triplet spin axis directions, as produced by replacement of chlorophyll *a* (Chl *a*) with non-native chlorophyll species (ZnChl *a* and BacterioChl *a*) in the reconstituted complexes, is unambiguously reflected in the polarization pattern of the carotenoid triplet state. For the first time, in the present investigation spin-polarization conservation has been shown to occur among natural cofactors in protein complexes during the TTET process. Proving the validity of the assumption of spin conservation adopted in the EPR spectral analysis, the results reinforce the hypothesis that in PCP proteins peridinin 614, according to X-ray nomenclature (Hofmann, E.; et al. *Science* **1996**, *272*, 1788−1791), is the carotenoid of election in the photoprotection mechanism based on TTET.

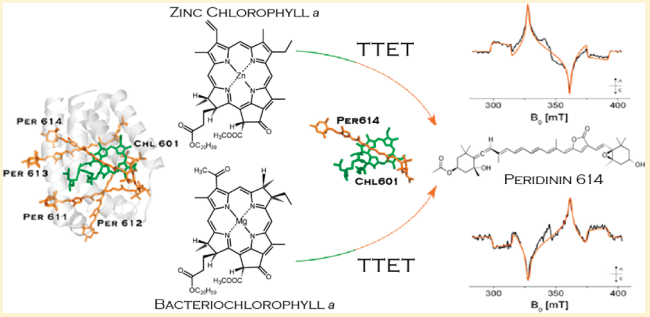

INTRODUCTION

Photosynthetic light harvesting is achieved by a variety of pigments, primarily (bacterio)chlorophylls and carotenoids, bound to distinct types of antenna proteins depending on the organisms. Unlike reaction centers, light-harvesting complexes differ substantially in terms of structure, pigment composition, and spectral properties.[1,2]

Marine algae contribute substantially to global CO_2 fixation. They possess efficient light-harvesting systems that in many species are optimized especially in the blue-green spectral region because water functions as a filter of both red and blue light. Many groups of marine eukaryotic algae employ carbonyl-substituted carotenoids, peridinin and fucoxanthin, in their light-harvesting strategy.

Dinoflagellates contain a unique soluble antenna, the peridinin−chlorophyll *a*−protein (PCP) complex, which differs from other antennas in using the carotenoid peridinin (Per) as the main light-harvesting pigment instead of chlorophyll (Chl). The high resolution X-ray structure of the main form of PCP (MFPCP) from the dinoflagellate *Amphidinium carterae* (*A. carterae*)[3] has been of great assistance in the understanding of the energy transfer pathways investigated by spectroscopic methods.[4−20]

The PCP antenna contains only Per and Chl *a* in a stoichiometric ratio of 4:1. The basic structure is a trimer. In each subunit of the trimer the pigments are arranged as two pseudoidentical domains of four Per molecules and one Chl *a* molecule; one such domain obtained by reconstitution of the N-terminal half of the protein is shown in Figure 1. The pigment clusters are located in the hydrophobic cavity formed by the protein. Distances between Per molecules within a single domain range from 4 to 11 Å, and the conjugated regions of the Per molecules are in van der Waals contact (3.3−3.8 Å) with the tetrapyrrole rings of the Chl

Received: July 21, 2011
Revised: September 21, 2011
Published: September 26, 2011

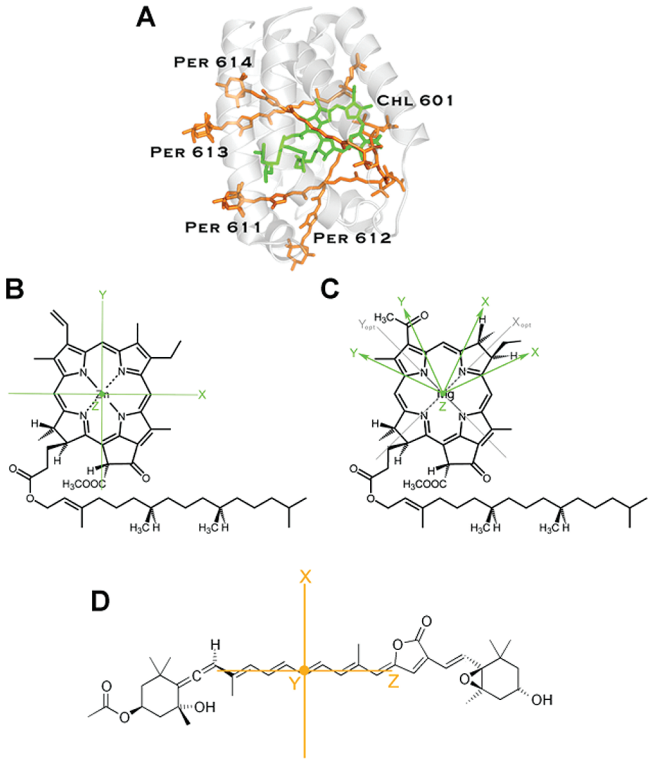

Figure 1. Structure of reconstituted PCP (A) derived from the coordinates deposited in the Brookhaven Protein Data Bank (3IIS) and molecular structures of ZnChl *a* (B), BChl *a* (C), and Per (D) with the orientation of the zero-field splitting tensor axes as defined in the text.

a molecules. The distance between the Mg atoms of the two Chl *a* molecules belonging to the two subclusters is 17.4 Å.

Along with the MFPCP, a minor component has also been reported which is eluted from an anion exchange column at high salt concentration. This form, denoted high-salt PCP (HSPCP), has 31% identity in amino acid sequence with MFPCP and contains two Chl *a* molecules but only six Per molecules.[21] The X-ray structure of HSPCP has been determined[22] and shows considerable similarity to the MFPCP structure in terms of pigment arrangement. HSPCP differs from MFPCP in the absence of two symmetry related Per molecules, called respectively PID612 and PID622 in the two subclusters, according to the nomenclature of Hofmann et al.[3] for MFPCP (Per612 in Figure 1 and the corresponding Per622 in the second subcluster).

The high-resolution structure determination has been coupled with pigment substitution through reconstitution or site-directed mutation of the PCP antenna in order to elucidate the details of the energy transfer among carotenoid and Chl pigments. For this purpose a heterologous expression system has been developed for the PCP apoprotein, which is then reconstituted with Per and a variety of Chl derivatives or bacteriochlorophyll *a* (BChl *a*) to obtain reconstituted PCP (RFPCP).[23,24] Heterochlorophyllous complexes, containing two different Chl's, have also been successfully produced.[25,26] Investigations by various optical spectroscopic techniques have demonstrated the excellent stability of RFPCP proteins, which maintain both high efficiency of the Per-to-Chl energy transfer function and the energy transfer pathways within the complex in the presence of non-native Chl derivatives.[7,13,23,27]

Recently, the X-ray structures of RFPCPs reconstituted with Chl *a*, Chl *b*, Chl *d*, and BChl *a* have been published.[28,29] The Chl *a* RFPCP complex does not deviate from the native PCP complex. The pigment arrangement is almost identical in all Chl RFPCPs, and the different Chl species replace Chl *a* almost perfectly, although a slight translational shift of BChl *a* in the Chl binding site has been observed (≈0.4 Å). No structural or spectroscopic information is available at the moment for ZnChl *a* RFPCP, but the same outcome is expected as for the other RFPCPs. A reorientation of the Chl ring is unlikely for ZnChl *a* because a replacement of the central Mg^{2+} by Zn^{2+} has been possible in many chlorophyll proteins and enzymes involved in chlorophyll metabolism without loss of functionality.[30]

Carotenoids bound to the light-harvesting complexes of bacteria, plants, and algae, having more than seven double bonds in the conjugated polyene chain, possess low-lying triplet states capable of trapping (B)Chl *a* triplet states by triplet−triplet energy transfer (TTET), thus avoiding the formation of the potentially harmful singlet oxygen.[31] In the case of dinoflagellates, the Per molecules in the isolated PCP complex satisfactorily play the photoprotective role, with a 100% efficiency in terms of TTET.[4,32]

Carotenoid triplet states formed in different antenna systems have been studied by means of several advanced magnetic resonance techniques: time-resolved electron paramagnetic resonance (TR-EPR), pulsed EPR, and double resonance techniques, i.e., pulsed electron−nuclear double resonance (ENDOR) and optically detected magnetic resonance. Among the different antenna systems investigated are the dinoflagellate PCP antenna including Chl *d* RFPCP,[9,12,14−16,18,19] LHCII (light harvesting complex II) of higher plants,[33] and the dinoflagellate intrinsic LHC.[34]

A common motif has been identified in the photoprotection strategy of the diverse antenna complexes adopting selected Chl *a*−carotenoid pairs for TTET. In the specific case of the PCP antenna, an exclusive path for triplet quenching in MFPCP has been postulated, involving Per 614/624 (PID614/PID624 in ref 3) as the quencher of the Chl *a* triplet states.[14,15,19] According to this mechanism, only one among the four Per molecules in van der Waals contact with each Chl *a* of the pigment cluster is devoted to photoprotection. The distinctive structural property for the selected Per is the presence of a water molecule coordinated to the central Mg atom of the donor, Chl *a*, at the interface between the donor−acceptor pair.

In this work we have extended and verified the validity of the spectroscopic approach adopted in previous investigations on the photoprotection mechanism in diverse antenna systems to PCP complexes reconstituted with ZnChl *a* or BChl *a*. The approach is based on the assumption of spin angular momentum conservation during TTET.[35−37] TTET takes place by an electron exchange mechanism, and since in the theoretical description no spin-dependent terms are explicitly considered, the spatial orientation of the triplet spin angular momentum must be conserved when resonance transfer occurs. If the molecular axes of the acceptor are rotated with respect to those of the donor molecule, the population probabilities of the donor triplet sublevels are transferred into the acceptor sublevels with relative probabilities given by the squared cosines of the angles relating the principal magnetic axes of the donor and the acceptor.[35−37]

The choice of ZnChl *a* and BChl *a* as possible donor molecules for TTET in the reconstituted proteins is determined

by the triplet state magnetic properties of these pigments, which can be used to verify the main assumption of spin conservation in all the previous EPR investigations on the antenna's photoprotection. ZnChl *a* is characterized by an initial spin polarization of the photoexcited triplet state which is distinct from that of Chl *a* due to a different selectivity in the intersystem-crossing (ISC) population of the triplet state spin sublevels attributed to the replacement of Mg by Zn in the Chl ring system.[38] Substitution of the central metal, while significantly affecting the ISC properties of the system, should have no effect on the structural and electronic properties of the Chl macrocycle,[39] conserving the directions of the zero-field-splitting (ZFS) axes. On the other hand, while the ISC populations of the BChl *a* triplet state are not altered significantly, the directions of the ZFS axes in the macrocycle are rotated with respect to those of the Chl *a* triplet state, due to the substantial change in spin density of the triplet state of the tetrahydroporphyrin compared to that of the dihydroporphyrin. Linear-dichroic (LD) absorbance-detected magnetic resonance (ADMR) studies have positioned the ZFS axes *X* and *Y* of BChl *a* at angles of ∼73° and ∼20° with respect to the optical axis corresponding to the Q_Y transition (Y_{opt}), while an angle of ∼45° has been found for the *X* and *Y* ZFS axes of Chl *a* with the Y_{opt} axis of Chl *a*.[40]

The effect produced on the polarization pattern of the donor triplet state by the substitution of the central metal ion or by axis rotation should be reflected on the acceptor triplet state according to spin conservation in a straightforward manner when the relative arrangement of the partners is maintained. This is the case for PCP proteins: the pigment arrangement is almost identical in all Chl RFPCPs and indistinguishable from that in MFPCP.[29]

In the present investigation we have demonstrated that indeed the variation of the donor triplet state properties is reflected in the spin-polarization pattern of the carotenoid triplet state as expected in the framework of spin angular momentum conservation. Proving the validity of the spectral analysis approach has allowed us to confirm the path proposed in previous works for triplet quenching in wild-type PCP proteins as well as the unique role of a special Per that is strongly coupled to the Chl *a* via an interfacial water molecule.

MATERIALS AND METHODS

Sample Preparation. RFPCP proteins were prepared according to Miller et al.[24] using a heterologously expressed N-domain PCP apoprotein, which dimerizes on reconstitution with Per and a wide range of Chl's. Per was extracted from PCP and purified by HPLC as previously described.[4] ZnChl *a* was prepared by metalation of pheophytin with zinc acetate in methanol.[41] BChl *a* was purchased from Sigma-Aldrich or extracted from *Rhodobacter sphaeroides*.[42]

The EPR samples of RFPCP were made to an optical density of ∼0.5/mm at the Chl Q_Y band. Oxygen was removed from the RFPCP samples by flushing with argon in the EPR capillary before freezing. Glycerol, previously degassed by several cycles of freezing, pumping, and thawing, was added (60% v/v) to obtain a transparent matrix.

The EPR samples of BChl *a* and ZnChl *a* were prepared by dissolving them in methyltetrahydrofuran (Me-THF) to a final Chl concentration of $\sim 10^{-5}$ M. They were sealed in a capillary tube after several pumping/freezing/thawing cycles in order to remove the oxygen from the sample. The solvent was distilled from sodium before usage.

TR-EPR Measurements. Experiments were performed on a Bruker Elexsys E580 pulsed EPR spectrometer at 9.7 GHz. Laser excitation at 532 nm (10 mJ/pulse and repetition rate of 10 Hz) was provided by the second harmonic of an Nd:YAG laser (Quantel Brilliant) in a Flexline dielectric resonator. The temperature was controlled by means of a helium cryostat (Oxford CF935) driven by a temperature controller (Oxford ITC503). TR-EPR experiments were performed in direct-detection mode, taking the signal directly from the mixer, without lock-in amplification with the SpecJet digitizer. Transients were accumulated both on and off resonance in order to eliminate the laser background signal by subtraction of the off-resonance traces. The transient signal rise time was about 50 ns. In the TR-EPR spectra, the integration period was 100−228 ns after the laser flash. The microwave power was 2 mW.

Spectral Analysis. Simulations of the powder spin-polarized triplet spectra were performed using the Easyspin[43] routine in Matlab. The program is based on the full diagonalization of the triplet state spin Hamiltonian, comprehensive of the Zeeman and magnetic dipole−dipole interactions. The line shape of the EPR spectrum is calculated assuming a powder distribution of molecular orientations with respect to the magnetic field direction. Triplet state input parameters are the relative population probabilities at zero field and the ZFS parameters *D* and *E*. The population probabilities in the applied field are linear combinations of the zero-field population rates with coefficients derived from the unitary transformation diagonalizing the spin Hamiltonian. The ordering of the triplet sublevels was chosen in agreement with previous studies: $|Z| > |X| > |Y|$ for ZnChl *a*,[40] $|Z| > |Y| > |X|$ for BChl *a*,[40] and $|Z| > |Y| > |X|$ for Per.[14]

The sublevel population probabilities of the acceptor (Per) triplet state were calculated with a home-written program in Matlab, according to the formalism of spin angular momentum conservation.[35−37] In the high field approximation the triplet population transfer occurring in the presence of the applied magnetic field can be calculated in the zero-field basis system and afterward converted in population probabilities in the applied field.[44] The zero-field population probabilities of the donor triplet sublevels (P_j^D) are transferred into the acceptor sublevels (P_i^A) with relative probabilities given by the squared cosines of the angles relating the principal magnetic axes of the donor and the acceptor:

$$P_i^A = \sum_j \cos^2 \vartheta_{ij} P_j^D$$

where ϑ_{ij} is the angle between the principal axis *j* of the donor and the axis *i* of the acceptor.

The resulting zero-field relative populations of the three sublevels were used as input parameters for the computation of the spectra in the simulation program for powder triplet state EPR spectra.

The directions of the ZFS axes of the Per triplet state were obtained applying the procedure of principal component analysis, using the Matlab function "princomp", to the X-ray coordinates of the Per molecules. The data set used in the calculations contained the spatial coordinates of the atoms of the conjugated chain of each Per molecule, as reported in the PDB files 3IIS and 2X21, respectively, for ZnChl *a* and BChl *a* RFPCP. The method is based on the solution of the covariance matrix of the data, in which the eigenvalues represent the amount

of variance attributed to each eigenvector. The resulting eigenvectors are a good approximation of the ZFS axes as determined in previous EPR investigations on a single crystal of β-carotene[45] and on deuterododecapentaenal in polyethylene film.[46] The solution vector with the greatest eigenvalue lies along the main axis (Z) of the Per molecule, the vector with the intermediate eigenvalue lies along the C−H bonds (Y), and the vector with the smallest eigenvalue is perpendicular to the molecular plane.

The directions of the ZFS axes of ZnChl *a* and BChl *a* used in the calculations were taken as defined in the literature for the Chl *a* and BChl *a* triplet states.[40,47] The relative orientation of the ZFS axes of donor and acceptor triplet states was determined considering the pigment arrangement in the X-ray structures of PCP reconstituted with Chl *a* (3IIS) for ZnChl *a* RFPCP and PCP reconstituted with BChl *a* (2X21) for BChl *a* RFPCP.

RESULTS

Photoexcited Triplet States in ZnChl *a* RFPCP. Figure 2 shows the X-band spin-polarized TR-EPR spectra of the donor triplet states, ^{T}ZnChl *a* and ^{T}Chl *a* in Me-THF glass, and those corresponding to the acceptor triplet states in Chl *a* RFPCP and ZnChl *a* RFPCPs shortly after the laser pulse. The triplet state TR-EPR spectra of the donor pigments have been successfully simulated as shown in the superimposed simulations in Figure 2 using the ZFS parameters and ISC population probabilities reported in Table 1, which are in agreement with literature values.[48] Different spin-polarization patterns have been detected for the two donor triplet states: an *eaeaea* polarization for ^{T}Chl *a* and an *aaeaee* pattern for ^{T}ZnChl *a*. As expected, the replacement of Mg with Zn leads to the enhancement of the Z spin sublevel population rate (corresponding to the out-of-plane molecular axes, see Figure 1) due to new spin−orbit coupling terms. The P_X and P_Y population rates are dominant for ^{T}Chl *a*, whereas P_Z is the dominant contribution to ISC for ^{T}ZnChl *a*.[38]

Inspection of the experimental TR-EPR spectra recorded for Chl *a* RFPCP and ZnChl *a* RFPCP reveals that the effect produced on the polarization pattern of the donor triplet state by the substitution of the central metal ion is clearly reflected in the acceptor triplet state polarization. While an *eaeaea* pattern has been detected for the Chl *a* RFPCP, an opposite polarization characterizes the ZnChl *a* RFPCP. The spin polarization of the acceptor triplet state populated in Chl *a* RFPCP is similar to that for MFPCP, as expected given the equivalence between the X-ray structures of MFPCP and RFPCP.[28]

The TR-EPR spectra can be simulated considering only one triplet state species with average ZFS parameters $|D|$ = 47.6 mT and $|E|$ = 4.6 mT. This allows a direct assignment to the Per molecule, on the basis of the comparison with the ZFS parameters reported in previous optically detected magnetic resonance and EPR studies performed on the MFPCP.[8,14]

Excitation of the Per singlet state by pulse-laser light at 532 nm is followed by rapid and highly efficient singlet−singlet energy transfer from the Per molecules to the Chl *a* in both MFPCP and RFPCP,[4,7,23] which can undergo intersystem crossing to form the ^{T}Chl *a*. The TTET from Chl *a* to Per in MFPCP occurs in about 17 ns.[4] Since the time resolution of the setup is about 50 ns, only the acceptor triplet state can be detected, as observed experimentally. The absence of any ^{T}Chl signal in the spectra proves that Per molecules play their photoprotective role in the quenching of the potentially harmful ^{T}Chl in the RFPCPs with 100% efficiency, as in the native PCP proteins. A small contribution from a radical species is present at the center of the TR-EPR spectra. This contribution has been neglected in the spectral analysis on the triplet state species.

The time evolution of the carotenoid triplet EPR spectrum is slow compared to its formation, 3−40 μs depending on the ZFS canonical orientation;[16] for this reason the spin polarization does not evolve significantly at short times after the laser pulse. The initial carotenoid polarization, detected by TR-EPR, has been analyzed in the framework of spin angular momentum conservation during TTET, as described in detail under Materials and Methods. The three sublevel populations of the donor triplet state are transferred into the acceptor sublevels with relative probabilities given by the squared cosines of the projections of the donor ZFS axes onto the acceptor axes.

Population probabilities for the Chl *a* and ZnChl *a* triplet states have been derived from simulations of the corresponding experimental TR-EPR spectra at a short time after the laser pulse. The absence of any donor triplet signal in the TR-EPR spectra of the RFPCPs, which is consistent with a TTET time on the order of tens of nanoseconds, allows us to state that the initial polarization pattern of the donor triplet state does not evolve significantly under the effect of spin relaxations before the transfer to the Per(s).

We have calculated the Per spectra for all four mutual Chl *a*−Per configurations derived from the X-ray structure of Chl *a* RFPCP,[28,29] as was previously done for MFPCP.[14] The corresponding results are shown in Figure 2, and the parameters are reported in Table 1 for both antenna complexes. The calculated spectra have the same polarization pattern as the corresponding experimental spectra only for two of the mutual arrangements of the Chl−Per pigment triplet axes present in the N-domain pigment subcluster of RFPCP. In both cases the selected arrangements correspond to the pairs (Zn)Chl *a*601−Per614 and (Zn)Chl *a*601−Per612.

An active role for Per612(622) in the TTET was ruled out in previous investigations on MFPCP and HSPCP by the fact that in the absence of these pigments, as in the HSPCP complex, the triplet state TR-EPR spectrum is exactly the same as for MFPCP.[15] The contribution of both Per612(622) and Per614(624) triplet states in MFPCP should affect the polarization pattern compared to the one corresponding to the sole Per614(624) triplet state in HSPCP, since the Chl−Per arrangement is different for the two pairs and consequently also the spin polarization is different as demonstrated by spectral calculations. For this reason, the polarization of the TR-EPR spectrum for MFPCP must be due to the Per614(624) triplet state exclusively. This argument can be used to exclude the (Zn)Chl *a*601−Per612 pair in the present analysis, based on the equivalence of the X-ray structures of MFPCP and RFPCPs and of the energy transfer pathways.[7,22,23] The outcome of the spectral analysis is that Per614 remains the best candidate for efficient triplet quenching not only in native PCP complexes (Per614/Per624) but also in RFPCP, as already demonstrated for Chl *d* RFPCP.[18] The intermediary role of other Per molecules in the TTET or the contribution of more than one Per triplet state to the TR-EPR spectrum has also been excluded.[14]

The agreement between the experimental and calculated triplet state TR-EPR spectra has been optimized by small rotations (±20°) around each of the ^{T}Per and ^{T}(Zn)Chl *a* ZFS axes, as initially determined by principal component analysis or oriented according to literature data,[40,47] considering only the (Zn)Chl *a*601−Per614 pair. The best agreement is obtained through simultaneous optimization of the correspondence between

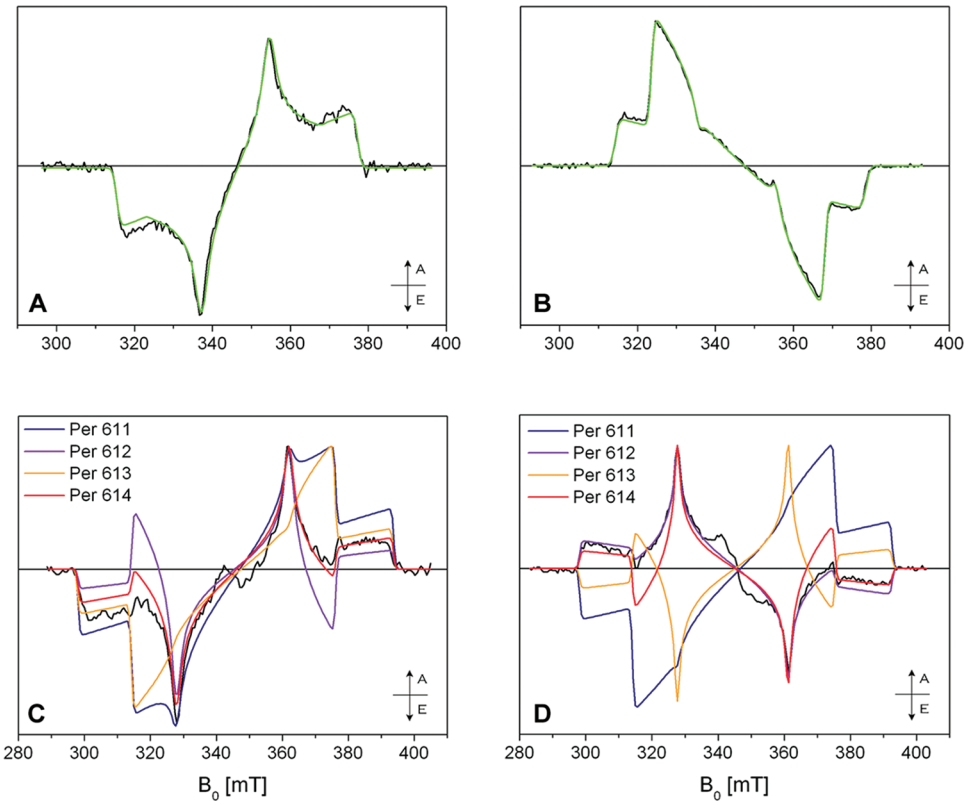

Figure 2. Experimental and simulated TR-EPR spectra of ^{T}Chl *a* (A) (adapted from ref 14) and ^{T}ZnChl *a* (B) in Me-THF glass at 90 K. Experimental TR-EPR spectrum of ^{T}Per for Chl *a* RFPCP (C) and ZnChl *a* RFPCP (D) at 150 K with the corresponding calculated EPR spectra for each Per surrounding the Chl donor. The simulation parameters are reported in Table 1. Order of energy for zero-field triplet sublevels: $|Z| > |X| > |Y|$ for ^{T}Chl *a* and $|Z| > |Y| > |X|$ for ^{T}Per. A = absorption; E = emission.

Table 1. Parameters for Triplet State Simulations[a]

Chl *a* in Me-THF glass		ZnChl *a* in Me-THF glass	
P_X	0.33	P_X	0.00
P_Y	0.56	P_Y	0.41
P_Z	0.11	P_Z	0.59
$D = 30.2 \pm 0.5$ mT		$D = 32.2 \pm 0.5$ mT	
$E = -4.4 \pm 0.1$ mT		$E = -4.1 \pm 0.1$ mT	
W_X:W_Y:W_Z = 2.0:2.0:2.0 mT		W_X:W_Y:W_Z = 1.5:1.5:2.0 mT	

Per molecules in Chl *a* RFPCP					Per molecules in ZnChl *a* RFPCP				
	Per611	Per612	Per613	Per614		Per611	Per612	Per613	Per614
P_X	0.28	0.15	0.35	0.14	P_X	0.33	0.57	0.14	0.54
P_Y	0.25	0.45	0.19	0.39	P_Y	0.25	0.28	0.44	0.21
P_Z	0.47	0.40	0.46	0.47	P_Z	0.42	0.15	0.42	0.25
$D = -47.90 \pm 0.75$ mT					$D = -47.30 \pm 0.75$ mT				
$E = -4.60 \pm 0.25$ mT					$E = -4.60 \pm 0.25$ mT				
W_X:W_Y:W_Z = 2.0:1.0:1.0 mT					W_X:W_Y:W_Z = 1.0:1.0:1.0 mT				

[a] P_X, P_Y, P_Z: zero-field populations of the triplet states. *D*, *E*: ZFS parameters. W_X, W_Y, W_Z: linewidths at the canonical positions in the EPR powder spectrum. Isotropic *g* value $g_{iso} = 2.0023$.

the calculated and experimental spectra for both reconstituted complexes. The result is reported in Figure 3 and corresponds to a 12° rotation of the ^{T}Per *X* and *Y* ZFS axes around the *Z* axis. The optimization satisfies also the spin-polarization pattern of the MFPCP TR-EPR spectrum, which does not differ from the one corresponding to RFPCP.[11,14] It must be noted that in the frame of the approximations used for the spectral analysis no relevance in terms of structural information can be given to the angular optimization.

Since computational methods available for the calculation of the ZFS tensor of triplet states are still not reliable in terms of the determination of the principal axes, the ^{T}Per ZFS axes have been determined by principal component analysis as explained in detail under Materials and Methods. Starting from the spectroscopic information available on the triplet state of β-carotene single crystal,[45] this method takes into account the effects produced by the distortion of the carbon skeleton induced by the protein surroundings. An optimization corresponding to a 12° rotation is within the range of uncertainty in the ZFS axis determination by principal component analysis.

The results for all the rotations of ±20° around the ZFS axes of both donor and acceptor triplet states are shown in the Supporting Information for the ZnChl *a*−Per614 pair in ZnChl *a* RFPCP. No significant variation of the spin-polarization pattern is produced, demonstrating that uncertainty in the directions of the ZFS axes does not affect the outcome of the spectral analysis.

Photoexcited Triplet States in BChl *a* RFPCP. Figure 4 shows the X-band spin-polarized TR-EPR spectra of the donor triplet state, ^{T}BChl *a* in Me-THF glass, and of the acceptor triplet state for BChl *a* RFPCP shortly after the laser pulse.

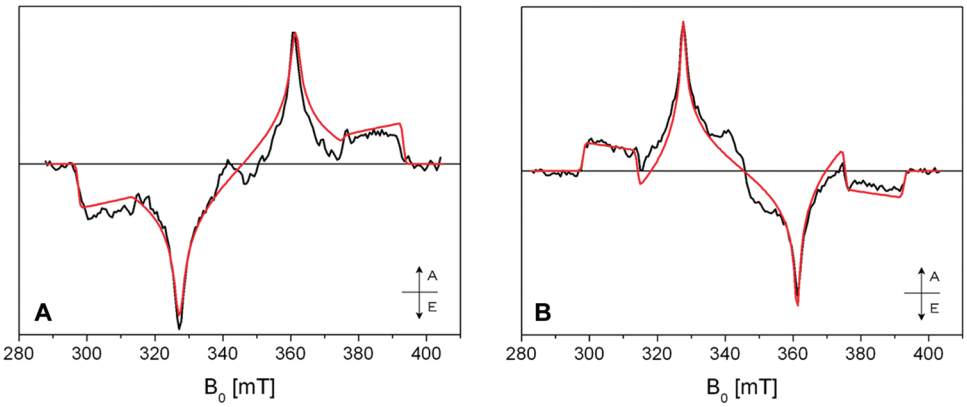

Figure 3. Experimental TR-EPR spectrum of ^{T}Per for Chl *a* RFPCP (A) and ZnChl *a* RFPCP (B) at 150 K with the corresponding calculated TR-EPR spectra of ^{T}Per614 after a 12° rotation of the Per's *X*, *Y* ZFS axes around the *Z* axis as described in the text. $|Z| > |Y| > |X|$. A = absorption; E = emission.

The spin-polarized TR-EPR spectrum of ^{T}BChl *a* in Me-THF glass has been simulated (Figure 4) using the ZFS parameters and ISC population probabilities indicated in Table 2, which are in perfect agreement with parameters previously reported.[48,49] The spin polarization is slightly different from that of ^{T}Chl *a* due to a small variation in the population probabilities and due to the sign inversion of the ZFS parameter *E*.[40,48]

As for Chl *a* RFPCP and ZnChl *a* RFPCP, the TR-EPR spectrum corresponding to BChl *a* RFPCP has been simulated considering only one triplet state species which can be directly assigned to the Per molecule.[8] The absence of any ^{T}BChl *a* contribution in the spectrum proves that the TTET process is characterized by 100% efficiency in this reconstituted protein as well. A small contribution from a radical species is present at the center of the TR-EPR spectra. This contribution has been neglected in the spectral analysis on the triplet state species.

The same approach used for the other reconstituted proteins has been adopted to analyze the initial carotenoid polarization in the framework of spin angular momentum conservation. We have calculated the Per spectra for all four mutual BChl *a*−Per configurations derived from the X-ray structure of BChl *a* RFPCP.[29] The corresponding results are reported in Figure 4 and the parameters are listed in Table 2.

In this case, the spectral analysis should reproduce the effects of a rotation of the triplet principal axes of the donor molecule compared to those of Chl *a* on the spin polarization of the acceptor triplet state. In fact, while the ISC populations of the ^{T}BChl *a* triplet state are not altered significantly, the ZFS axis directions in the macrocycle are rotated with respect to those of the ^{T}Chl *a* triplet state as proven experimentally.[40] LD-ADMR studies have defined the position of the ZFS axes *X* and *Y* of BChl *a* at angles of ∼73° and ∼20° with respect to the optical axis corresponding to the Q_Y transition, while an angle of ∼45° has been determined for the ZFS axes of Chl *a*. The LD-ADMR experiments allow only an estimation of the absolute angles between Y_{opt} and the *X* and *Y* axes, leaving two possible orientations of the ZFS axes with respect to the molecular axes (see Figure 4). This ambiguity has been removed only for the ZFS axes of ^{T}Chl *a* in a pulse ENDOR investigation on the photoexcited ^{T}Chl *a*.[47] An analogous ENDOR study on the photoexcited ^{T}BChl *a*, although assuming a precise orientation for the data analysis, does not remove the ambiguity.[49] For this reason the spectral analysis has been carried out for both positive and negative angles with respect to the optical axes.

The carotenoid spin polarization detected for BChl *a* RFPCP does not differ significantly from the corresponding polarization found for MFPCP and Chl *a* RFPCP despite the expected rotation of the in-plane triplet axes for ^{T}BChl *a* compared to that of ^{T}Chl *a*. This is due to the small differences between the population probabilities P_X and P_Y of the donor triplet state which are therefore not very sensible to the rotation around the *Z* ZFS axes in terms of acceptor sublevel projections.

The outcome of the analysis is perfectly in line with the results obtained for MFPCP and for (Zn)Chl *a* RFPCP; the spin-polarization pattern is reproduced only for two mutual arrangements of the BChl *a*−Per triplet axes. Exclusion of the BChl *a*601−Per612 pair, on the basis of the results on HSPCP, allows us to select the BChl *a*601−Per614 pair as the best arrangement in terms of triplet axis orientations. The projections of the donor population probabilities into the acceptor sublevels according to the relative arrangement of the triplet axes for the BChl *a*601−Per614 pair satisfactorily reproduce the carotenoid experimental spin polarization, in perfect agreement with all the other results.[14]

The ambiguity regarding the sign of the angle between the optical and magnetic axes does not significantly alter the results. Figure 4 shows very similar trends for the four pairs of donor−acceptor pigments for both positive (20°) and negative angles (−20°) between the in-plane triplet axes and optical axes of ^{T}BChl *a*. Since these angles are also defined with a great uncertainty (±15°), the spectra have been calculated for different angles to find the best correspondence between the calculated and experimental spectra for the three BChl *a*−Per pairs. The results, available in the Supporting Information, prove that the uncertainty in the directions of the donor's in-plane ZFS axes does not affect the outcome of the spectral analysis since there is no significant variation of the spin-polarization pattern of either BChl *a*−Per pair. The best agreement is still obtained for the BChl *a*601−Per614 pair, as for native PCP and the other RFPCP complexes.[14]

In Figure 5 the experimental TR-EPR spectrum for BChl *a* RFPCP has been compared to the calculated spectra of ^{T}Per614 for the optimized orientation of the carotenoid triplet axes, reported for (Zn)Chl *a* RFPCP in Figure 3 (+12° around the *Z* axis), while varying the in-plane ZFS axes of ^{T}BChl *a* in a 30° interval, according to the uncertainty given in the axis orientation, around each of the two possible orientations reported in ref

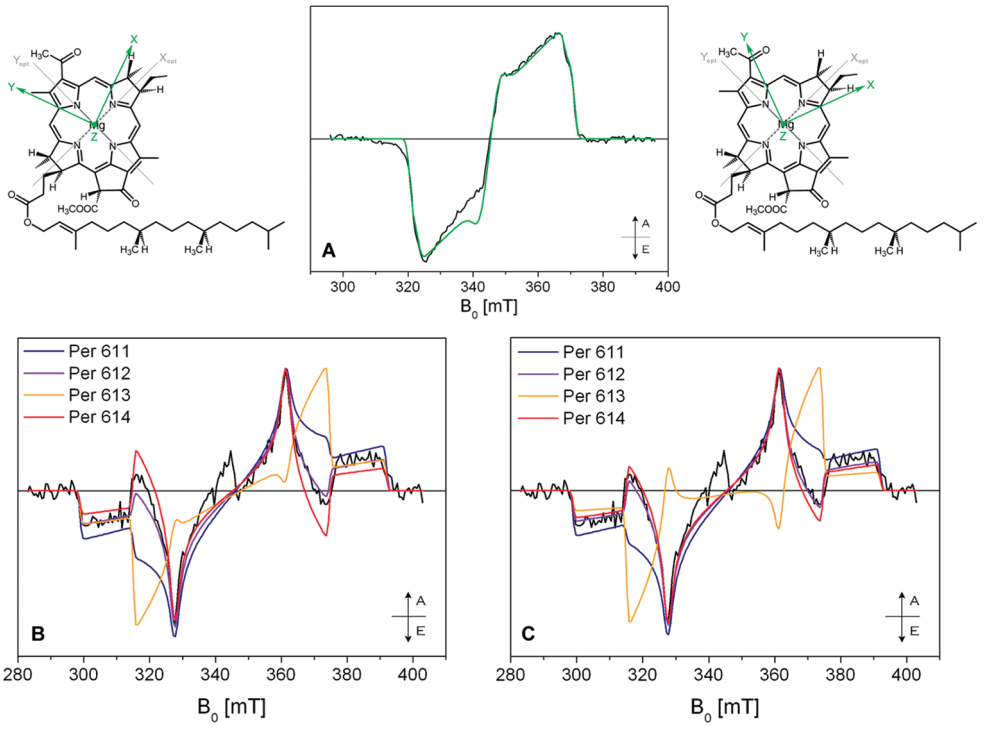

Figure 4. Experimental and simulated TR-EPR spectra of ^{T}BChl *a* in Me-THF glass at 90 K (A). Experimental TR-EPR spectrum of ^{T}Per for BChl *a* RFPCP at 150 K and calculated EPR spectra for each Per surrounding the Chl donor and for two possible orientations of the donor's in-plane ZFS axes:[40] at angles of −20° (B) and +20° (C) with respect to the corresponding optical axes (X_{opt} and Y_{opt}). The molecular structures with the two possible orientations of the ZFS axes are shown above the corresponding spectra. The simulation parameters are reported in Table 2. $|Z| > |Y| > |X|$ for ^{T}BChl *a*; $|Z| > |Y| > |X|$ for ^{T}Per. A = absorption; E = emission.

Table 2. Parameters for Triplet State Simulations[a]

BChl *a* in Me-THF glass									
P_X	0.44								
P_Y	0.40								
P_Z	0.16								
D = 25.25 ± 0.5 mT									
E = 6.55 ± 0.1 mT									
W_X:W_Y:W_Z = 4.0:2.0:2.0 mT									
Per molecules in BChl *a* RFPCP									
	−20°[b]					+20°[b]			
	Per611	Per612	Per613	Per614		Per611	Per612	Per613	Per614
P_X	0.29	0.20	0.36	0.19	P_X	0.31	0.19	0.38	0.19
P_Y	0.32	0.37	0.26	0.41	P_Y	0.33	0.39	0.26	0.40
P_Z	0.39	0.43	0.38	0.40	P_Z	0.36	0.42	0.36	0.41
D = −46.60 ± 0.75 mT									
E = −4.30 ± 0.25 mT									
W_X:W_Y:W_Z = 2.0:1.0:1.0 mT									

[a] P_X, P_Y, P_Z: zero-field populations of the triplet states. D, E: ZFS parameters. W: linewidths at the canonical positions in the EPR powder spectrum. Isotropic g value g_{iso} = 2.0023. [b] Orientation of the X and Y ZFS axes of BChl *a* with respect to the corresponding optical axes (X_{opt} and Y_{opt}).

40. The best agreement is obtained for the negative angles between the in-plane triplet axes and optical axes of ^{T}BChl a, removing in this way the ambiguity on the clockwise versus counterclockwise reorientation of the triplet axes, in accord with the triplet axis orientation assumed in a previous ENDOR study on ^{T}BChl *a* in vitro.[49]

DISCUSSION

Structure−function relationships in native proteins are an important goal for biophysical studies. Structure is heavily based on X-ray analysis at atomic resolution, while function is often revealed by the complementary use of optical or magnetic spectroscopy. While advanced EPR techniques have been frequently applied to photosynthetic reaction center proteins and have revealed important details of the electron transfer process in photosynthesis,[50] they have not been used to the same extent in the structure−function investigation of antenna proteins.[14,18,33,34] Identification of the pigments involved in the TTET from Chl molecules to carotenoids is an important issue related to the photoprotective function of carotenoids in the light-harvesting complexes of the photosynthetic apparatus.

TTET, based on Dexter's exchange mechanism, requires stringent distance and geometric conditions in the arrangement of the partners. The electronic coupling V_{TT}, which governs the rate of energy transfer, depends on the two-electron exchange integral involving the LUMO and the HOMO of the donor and acceptor and is thus extremely sensitive to the mutual orientation of the molecular π orbitals of the molecules involved. Even small differences in the mutual orientation, and in the distance between the π orbitals of a donor−acceptor pair, may lead to substantial variations in triplet quenching. In multichromophoric systems

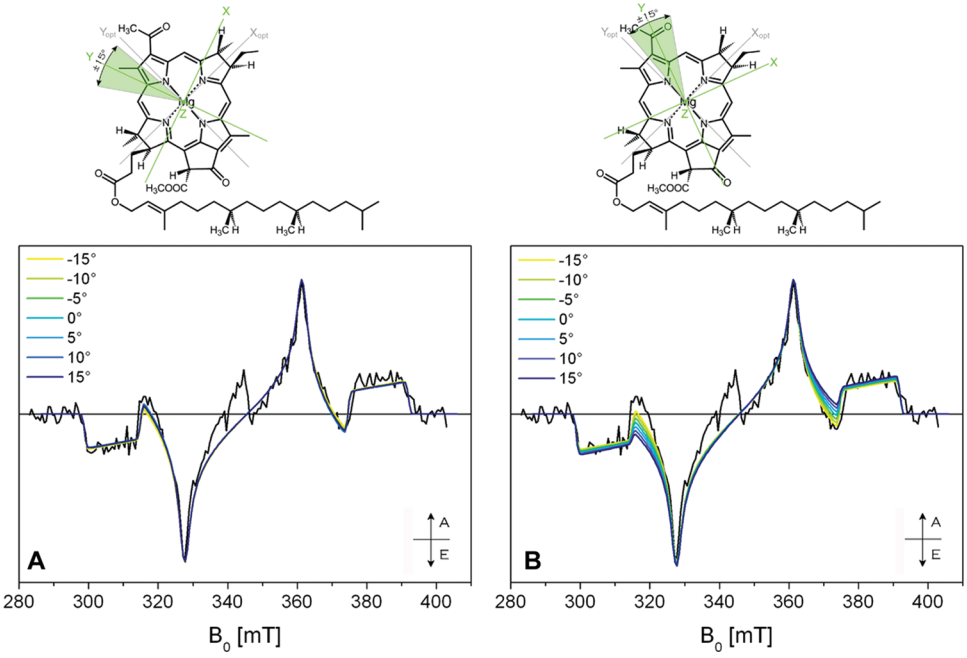

Figure 5. Experimental TR-EPR spectrum for BChl *a* RFPCP at 150 K and calculated EPR spectra of ^{T}Per614, for different orientations of the in-plane ZFS axes of ^{T}BChl *a* in a 30° interval around the two possible orientations of the ZFS *X* and *Y* axes: at −20° (A) and at +20° (B) with respect to the corresponding optical axes as reported in ref 40. The interval of considered angles is depicted above with respect to the molecular structure. The *X* and *Y* ZFS axes of ^{T}Per are rotated +12° around *Z* as in Figure 3. $|Z| > |Y| > |X|$. A = absorption; E = emission.

such as PCP, this can result in preferential pathways. The presence of several Per molecules at comparable van der Waals distances from the conjugated Chl *a* macrocycle[3] complicates the analysis of the TTET pathways and requires input from spectroscopic tools. In previous works, we addressed this question and we identified individual pairs of pigments involved in TTET not only in the PCP proteins but also in other antenna complexes, LHCII from higher plants and LHC from the dinoflagellate *A. cartarae*.[14,15,18,33,34]

We have shown that by exploiting the spin angular momentum conservation condition, which is an intrinsic property of the electron exchange mechanism, it is possible to gain insight into the structural requirements of TTET. Spin conservation is fulfilled only if[37]

(a) the TTET transfer results from a pure electrostatic exchange mechanism and not from magnetic type interactions,
(b) spin−orbit interactions are negligible in both the donor and acceptor molecules, and
(c) the transfer occurs on a time scale which allows spin alignment with respect to the external magnetic field; in X-band EPR this occurs for times longer than 20 ps.

In systems where any of these assumptions becomes invalid, the spin directions are not necessarily conserved during the energy transfer. In the past, spin angular momentum conservation has been experimentally confirmed for many systems at zero field and in the presence of an external magnetic field, both in single crystals and in randomly oriented systems.[35,51,52] In a few cases the spin-polarization conservation was not confirmed because of dynamic complications such as fast TTET or intervention of excited triplet states.[53] Since the Per triplet rise time is 17 ns,[4] the condition of spin alignment is definitely satisfied, but the other conditions have not been verified for large molecular systems such as Chl−carotenoid pairs and in the presence of heavy nuclei as in Chl species. The complexity of the problem compared to previous investigations is intrinsic in the biological relevance of the systems under investigation.

In the present study we have further addressed the question of TTET in antenna complexes by using PCP proteins reconstituted with Chl pigments that were opportunely selected in order to verify the consistency of our spectroscopic approach.[14] Among the possible Chl's suitable to take the role of donors in TTET, ZnChl *a* and BChl *a* are both characterized by triplet state properties which differ from those of Chl *a* in a manner that allows verification of spin angular momentum conservation during the transfer mechanism. ZnChl *a* is characterized by a different selectivity in the ISC population of the triplet state spin sublevels compared to Chl *a*.[38] On the other hand, while the ISC populations of the BChl *a* triplet state are not altered significantly, the directions of the ZFS axes in the macrocycle are rotated with respect to those of the Chl *a* triplet state.[40] Indeed, even a simple and qualitative inspection of the TR-EPR spectra of the Chl *a* and ZnChl *a* triplet states and of the corresponding RFPCPs reveals that the inversion of the spin-polarization pattern in the donor spectra is reflected in the spin polarization of the acceptor triplet state in the RFPCPs. The spin polarization for ZnChl *a* RFPCP is reproduced by the same arrangements of pigments selected in the investigation on MFPCP,[14] despite the important variation of spin polarization induced by the substitution of the central metal ion. This is a strong evidence that the condition of spin-polarization conservation is satisfied for the systems under investigation.

The spectral effects produced by the triplet axis rotation when comparing Chl *a* and BChl *a* RFPCPs are not as straightforward, but the spectral analysis, which has been made in parallel to that for Chl *a* and ZnChl *a* RFPCPs, is perfectly consistent in the framework of spin conservation, selecting the same donor−acceptor

pair (Chl 601−Per614) in all three RFPCP antenna complexes under investigation, and in perfect agreement with previous results on PCP proteins.[14,18]

For all these reasons, the TR-EPR study shows unequivocally that the initial polarization of the donor triplet state is projected into the acceptor triplet state according to the relative spin axis directions of the two molecules involved in TTET, in the frame of spin conservation. It is worth noting that this result does not depend critically on the assumptions that have been made to perform the spectral analysis. While the donor populations have been derived directly from simulations of the experimental TR-EPR spectra of the donor triplet state populated via ISC in organic solvent, the ZFS principal axis directions have been derived from literature data on Chl molecules in solution.[40] Two spin-polarization patterns for the Chl *a* triplet state in vitro have been reported in the literature depending on the polarity of the solvent and the ligation state of Mg^{2+}.[54−56] The spin-polarization pattern for the Chl's in the antenna complex will belong to one of the two sets. In the previous spectroscopic study on MFPCP, it has been verified that the same conclusions can be drawn from the analysis for both sets of population probabilities.[14] On the other hand, conservation of the ZFS axis directions between Chl *a* in vitro and Chl *a* in the protein environment, at least for the primary donor ^{T}P680 of photosystem II, have been proven by ENDOR spectroscopy.[47]

For ZnChl *a* RFPCP the assumption has been made that the triplet axis directions of the ZnChl *a* triplet state are not varied compared to those of Chl *a* on the basis of ENDOR studies on the corresponding radical cations.[39] In this investigation no significant alteration of the spin density was found in the zinc-substituted compound, proving that the electron density of the HOMO is not influenced by the metal substitution.

According to our calculations, the inaccuracy which might derive from the uncertainty of the triplet axis direction of both the BChl and Per triplet states does not change significantly the calculated spin polarization for the Per614 triplet state, and thus the outcome of the spectral analysis.

CONCLUSIONS

The present results on RFPCP clearly show spin-polarization conservation among Chl−carotenoid cofactors in light-harvesting complexes. This is the first time that spin conservation during TTET has been verified in protein complexes.

Validating the correctness of the spectroscopic approach adopted in the characterization of the TTET pathways in antenna complexes, the present investigation also strengthens the conclusions drawn in the previous EPR investigations on this topic.[14,16,18,33,34] Since spin conservation is fulfilled, localization of the triplet state on one specific Per (Per614/624) out of four in each of the two pigment subclusters of PCP has been definitely confirmed. As previously pointed out, the specific Per−Chl pair involved in the photoprotective mechanism is characterized by the shortest center-to-center distance and by the presence of an interfacial water molecule which is coordinated to the central Mg atom of Chl *a*. This water molecule is present in all RFPCPs whose X-ray structural data are available.[22,29] There is no reason to expect a different structural motif for ZnChl *a* RFPCP, since among the divalent metals Zn is considered the most suited to replace Mg without affecting the structural and coordination properties of the porphyrin macrocycle.[39] Further experiments on MFPCP are underway to explore the role of the bridging molecule, which is an unique feature of the identified photoprotective pair of pigments.

Finally, the spectroscopic approach, based on spin conservation, can be adopted to study the photosynthetic light-harvesting complexes of unknown structure in order to validate or propose a structural model for the pigment arrangement.[19] The extension of this approach to artificial antenna complexes, where not only Chl's but also carotenoids are incorporated in the artificial architectures, would gain insight into the structural information on the donor−acceptor relative orientation.[57,58] The structural requirements for efficient TTET should be considered when designing new biomimetic compounds since photoprotection might play an important role in extending the lifetime of devices under prolonged and widespread illumination conditions.

ASSOCIATED CONTENT

Supporting Information. Additional figures are presented showing the effects of the rotation in the range ±20° around each of the ^{T}Per, ^{T}ZnChl *a*, and ^{T}BChl *a* ZFS axes, as determined by multicomponent analysis or as directed on the basis of literature data,[40] on the outcome of the calculation for the ZnChl *a*−Per614 pair in ZnChl *a* RFPCP and for the BChl *a*−Per614 pair in BChl *a* RFPCP. For rotation around the *Z* ZFS axis of ^{T}BChl *a*, the BChl *a*−Per611 and BChl *a*−Per613 pairs are also shown. This material is available free of charge via the Internet at http://pubs.acs.org.

AUTHOR INFORMATION

Corresponding Author

*E-mail: marilena.divalentin@unipd.it. Tel.: +39 049 827 5139.

ACKNOWLEDGMENT

This work was supported by MIUR under the project PRIN2008 (prot. 20088NTBKR_004).

REFERENCES

(1) *Oxygenic Photosynthesis: The Light Reactions*; Ort, D. R., Yocum, C. F., Eds.; Kluwer Academic Publishers: Dordrecht, The Netherlands, 1996; Vol. 4.

(2) van Amerongen, H.; Valkunas, L.; van Grondelle, R. *Photosynthetic Excitons*; World Scientific: River Edge, NJ, 2000.

(3) Hofmann, E.; Wrench, P. M.; Sharples, F. P.; Hiller, R. G.; Welte, W.; Diederichs, K. *Science* **1996**, *272*, 1788–1791.

(4) Bautista, J. A.; Hiller, R. G.; Sharples, F. P.; Gosztola, D.; Wasielewski, M.; Frank, H. A. *J. Phys. Chem. A* **1999**, *103*, 2267–2273.

(5) Krueger, B. P.; Lampoura, S. S.; van Stokkum, I. H. M.; Papagiannakis, E.; Salverda, J. M.; Gradinaru, C. C.; Rutkauskas, D.; Hiller, R. G.; van Grondelle, R. *Biophys. J.* **2001**, *80*, 2843–2855.

(6) Zigmantas, D.; Hiller, R. G.; Sundstrom, V.; Polivka, T. *Proc. Natl. Acad. Sci. U.S.A.* **2002**, *99*, 16760–16765.

(7) Ilagan, R. P.; Chapp, T. W.; Hiller, R. G.; Sharples, F. P.; Polivka, T.; Frank, H. A. *Photosynth. Res.* **2006**, *90*, 5–15.

(8) Carbonera, D.; Giacometti, G.; Agostini, G. *Spectrochim. Acta, Part A* **1995**, *51*, 115–123.

(9) Carbonera, D.; Giacometti, G.; Segre, U. *J. Chem. Soc., Faraday Trans.* **1996**, *92*, 989–993.

(10) Krikunova, M.; Lokstein, H.; Leupold, D.; Hiller, R. G.; Voigt, B. *Biophys. J.* **2006**, *90*, 261–271.

(11) Polivka, T.; Hiller, R. G.; Frank, H. A. *Arch. Biochem. Biophys.* **2007**, *458*, 111–120.

(12) Niklas, J.; Schulte, T.; Prakash, S.; van Gastel, M.; Hofmann, E.; Lubitz, W. *J. Am. Chem. Soc.* **2007**, *129*, 15442–15443.
(13) Wörmke, S.; Mackowski, S.; Brotosudarmo, T. H. P.; Jung, C.; Zumbusch, A.; Ehrl, M.; Scheer, H.; Hofmann, E.; Hiller, R. G.; Bräuchle, C. *Biochim. Biophys. Acta* **2007**, *1767*, 956–964.
(14) Di Valentin, M.; Ceola, S.; Salvadori, E.; Agostini, G.; Carbonera, D. *Biochim. Biophys. Acta* **2008**, *1777*, 186–195.
(15) Di Valentin, M.; Ceola, S.; Salvadori, E.; Agostini, G.; Giacometti, G. M.; Carbonera, D. *Biochim. Biophys. Acta* **2008**, *1777*, 1355–1363.
(16) Di Valentin, M.; Ceola, S.; Agostini, G.; Giacometti, G. M.; Angerhofer, A.; Crescenzi, O.; Barone, V.; Carbonera, D. *Biochim. Biophys. Acta* **2008**, *1777*, 295–307.
(17) van Stokkum, I. H. M.; Papagiannakis, E.; Vengris, M.; Salverda, J. M.; Polivka, T.; Zigmantas, D.; Larsen, D. S.; Lampoura, S. S.; Hiller, R. G.; van Grondelle, R. *Chem. Phys.* **2009**, *357*, 70–78.
(18) Di Valentin, M.; Agostini, G.; Salvadori, E.; Ceola, S.; Giacometti, G. M.; Hiller, R. G.; Carbonera, D. *Biochim. Biophys. Acta* **2009**, *1787*, 168–175.
(19) Di Valentin, M.; Salvadori, E.; Ceola, S.; Carbonera, D. *Appl. Magn. Reson.* **2010**, *37*, 191–205.
(20) Bonetti, C.; Alexandre, M. T. A.; van Stokkum, I. H. M.; Hiller, R. G.; Groot, M. L.; van Grondelle, R.; Kennis, J. T. M. *Phys. Chem. Chem. Phys.* **2010**, *12*, 9256–9266.
(21) Sharples, F. P.; Wrench, P. M.; Ou, K. L.; Hiller, R. G. *Biochim. Biophys. Acta* **1996**, *1276*, 117–123.
(22) Schulte, T.; Sharples, F. P.; Hiller, R. G.; Hofmann, E. *Biochemistry* **2009**, *48*, 4466–4475.
(23) Polivka, T.; Pascher, T.; Sundstrom, V.; Hiller, R. G. *Photosynth. Res.* **2005**, *86*, 217–227.
(24) Miller, D. J.; Catmull, J.; Puskeiler, R.; Tweedale, H.; Sharples, F. P.; Hiller, R. G. *Photosynth. Res.* **2005**, *86*, 229–240.
(25) Brotosudarmo, T. H. P.; Hofmann, E.; Hiller, R. G.; Wörmke, S.; Mackowski, S.; Zumbusch, A.; Bräuchle, C.; Scheer, H. *FEBS Lett.* **2006**, *580*, 5257–5262.
(26) Brotosudarmo, T. H. P.; Mackowski, S.; Hofmann, E.; Hiller, R. G.; Bräuchle, C.; Scheer, H. *Photosynth. Res.* **2008**, *95*, 247–252.
(27) Mackowski, S.; Wörmke, S.; Brotosudarmo, T. H. P.; Scheer, H.; Bräuchle, C. *Photosynth. Res.* **2008**, *95*, 253–260.
(28) Schulte, T.; Niedzwiedzki, D. M.; Birge, R. R.; Hiller, R. G.; Polivka, T.; Hofmann, E.; Frank, H. A. *Proc. Natl. Acad. Sci. U.S.A.* **2009**, *106*, 20764–20769.
(29) Schulte, T.; Hiller, R. G.; Hofmann, E. *FEBS Lett.* **2010**, *584*, 973–978.
(30) *Chlorophylls and Bacteriochlorophylls Biochemistry, Biophysics, Functions and Applications*; Grimm, B., Porra, R. J., Rüdiger, W., Scheer, H., Eds.; Springer: Dordrecht, 2006; Vol. 25.
(31) Frank, H. A.; Cogdell, R. J. *Photochem. Photobiol.* **1996**, *63*, 257–264.
(32) Schulte, T.; Johanning, S.; Hofmann, E. *Eur. J. Cell Biol.* **2010**, *89*, 990–997.
(33) Di Valentin, M.; Biasibetti, F.; Ceola, S.; Carbonera, D. *J. Phys. Chem. B* **2009**, *113*, 13071–13078.
(34) Di Valentin, M.; Salvadori, E.; Agostini, G.; Biasibetti, F.; Ceola, S.; Hiller, R.; Giacometti, G. M.; Carbonera, D. *Biochim. Biophys. Acta* **2010**, *1797*, 1759–1767.
(35) El-Sayed, M. A.; Tinti, D. E.; Yee, E. M. *J. Chem. Phys.* **1969**, *51*, 5721–5723.
(36) El-Sayed, M. A. *J. Chem. Phys.* **1971**, *54*, 680–692.
(37) Brenner, H. C.; Brock, J. C.; Harris, C. B. *Chem. Phys.* **1978**, *31*, 137–164.
(38) Clarke, R. H.; Connors, R. E.; Schaafsma, T. J.; Kleibeuker, J. F.; Platenkamp, R. J. *J. Am. Chem. Soc.* **1976**, *98*, 3674–3677.
(39) Käß, H.; Lubitz, W.; Hartwig, G.; Scheer, H.; Noy, D.; Scherz, A. *Spectrochim. Acta, Part A* **1998**, *54*, 1141–1156.
(40) Vrieze, J.; Hoff, A. J. *Chem. Phys. Lett.* **1995**, *237*, 493–501.
(41) Fischer, H.; Orth, H. *Die Chemie des Pyrrols*; Akademische Verlagsgesellschaft: Leipzig, 1940; Vol. II/2.
(42) Struck, A.; Cmiel, E.; Katheder, I.; Scheer, H. *FEBS Lett.* **1990**, *268*, 180–184.
(43) Stoll, S.; Schweiger, A. *J. Magn. Reson.* **2006**, *178*, 42–55.
(44) Kobori, Y.; Fuki, M.; Murai, H. *J. Phys. Chem. B* **2010**, *114*, 14621–14630.
(45) Frick, J.; Von Schütz, J. U.; Wolf, H. C.; Kothe, G. *Mol. Cryst. Liq. Cryst.* **1990**, *183*, 269–272.
(46) Kok, P.; Groenen, E. J. J. *J. Am. Chem. Soc.* **1996**, *118*, 7790–7794.
(47) Lendzian, F.; Bittl, R.; Telfer, A.; Lubitz, W. *Biochim. Biophys. Acta* **2003**, *1605*, 35–46.
(48) Angerhofer, A. Chlorophyll Triplets and Radical Pairs. In *Chlorophylls*; Scheer, H. Ed.; CRC Press: Boca Raton, FL, 1991; pp 945−992.
(49) Marchanka, A.; Lubitz, W.; van Gastel, M. *J. Phys. Chem. B* **2009**, *113*, 6917–6927.
(50) Lubitz, W. EPR in Photosynthesis. In *Electron Paramagnetic Resonance. Specialist Periodical Reports*; Gilbert, B. C., Davies, M. J., Eds.; Royal Society of Chemistry: Cambridge, U.K., 2004; Vol. 19, pp 174−224.
(51) Imamura, T.; Onitsuka, O.; Murai, H.; Obi, K. *J. Phys. Chem.* **1984**, *88*, 4028–4031.
(52) Akiyama, K.; Terokubota, S.; Ikoma, T.; Ikegami, Y. *J. Am. Chem. Soc.* **1994**, *116*, 5324–5327.
(53) Kim, S. S. *J. Chem. Phys.* **1978**, *68*, 333–334.
(54) Thurnauer, M. C. *Rev. Chem. Intermed.* **1979**, *3*, 197–230.
(55) Clarke, R. H.; Hotchandani, S.; Jagannathan, S. P.; Leblanc, R. M. *Chem. Phys. Lett.* **1982**, *89*, 37–40.
(56) Clarke, R. H. *Triplet State ODMR Spectroscopy: Techniques and Applications to Biophysical Systems*; Clarke, R. H., Ed.; Wiley: New York, 1982.
(57) Carbonera, D.; Di Valentin, M.; Agostini, G.; Giacometti, G.; Liddell, P. A.; Gust, D.; Moore, A. L.; Moore, T. A. *Appl. Magn. Reson.* **1997**, *13*, 487–504.
(58) Carbonera, D.; Di Valentin, M.; Corvaja, C.; Giacometti, G.; Agostini, G.; Liddell, P. A.; Moore, A. L.; Moore, T. A.; Gust, D. *J. Photochem. Photobiol., A* **1997**, *105*, 329–335.